

Let us consider first the frictional contribution; this is given by

$$\left(\frac{\partial F'}{\partial t}\right)_{cl} = \frac{-1}{\Omega} \int d\mathbf{V} \exp(-i\delta \cdot \mathbf{V}) \int_{-\infty}^{\phi} d\phi' \times \exp[-\alpha(\phi - \phi')] \frac{\partial}{\partial \mathbf{V}'} \cdot [\langle \Delta \rangle_{0i} f'(\mathbf{V}')]. \quad (\text{A2})$$

On substituting for $\langle \Delta \rangle_{0i}$ from Eq. (7) and on using the relation

$$\int d\mathbf{V} f_{0i}(\mathbf{V}) \exp(-i\xi \cdot \mathbf{V}) = \exp[-\frac{1}{2}(\xi^2 V_0^2)],$$

Eq. (A2) can be written as

$$\left(\frac{\partial F'}{\partial t}\right)_{cl} = -\frac{iN\Gamma\mu}{2\Omega\pi^2} \int d\mathbf{V} \exp(-i\delta \cdot \mathbf{V}) \int d\phi' \times \exp[-\alpha(\phi - \phi')] \frac{\partial}{\partial \mathbf{V}'} \cdot \left\{ f'(\mathbf{V}') \int d\xi \frac{\xi}{\xi^2} \times \exp[i\xi \cdot \mathbf{V}' - \frac{1}{2}(\xi^2 V_0^2)] \right\}. \quad (\text{A3})$$

Now if we use Eq. (16) to zeroth order for $f'(\mathbf{V}')$ for

the right-handed polarized wave, Eq. (A3) after some simplifications goes over to

$$\left[\left(\frac{\partial F'}{\partial t}\right)_{cl}\right]_{F=F_0} = -\left(\frac{N\Gamma\mu\Lambda}{4\pi^2\Omega v_0^2}\right) \int d\mathbf{V} V_{\perp} \exp(-i\delta \cdot \mathbf{V}) \times \int_{-\infty}^{\phi} d\phi' f_{0e}(\mathbf{V}') \exp[-\alpha(\phi - \phi')] \int_0^{\infty} dt \times \exp[-\Omega(\alpha - i)t] \exp(-i\phi') \int \frac{d\xi}{\xi^2} \times \exp[i\xi \cdot \mathbf{V}' - \frac{1}{2}(V_0^2 \xi^2)] \left(\frac{\partial F}{\partial \sigma_x} + \frac{i\partial F}{\partial \sigma_y}\right)_{\delta=0} \times \left\{ i\xi^2 - \frac{(\mathbf{V}' \cdot \xi)}{v_0^2} - ik t \xi_z + \frac{\xi_{\perp}}{V_{\perp}} \exp[i(\phi' - \theta)] \right\} + N\Gamma Q_1', \quad (\text{A4})$$

where Q_1' is defined by Eq. (34). Equation (A4) can be immediately rewritten in the form of Eq. (33). Proceeding on the similar lines, the other elements of $(\partial F'/\partial t)_{cl}$ can be easily evaluated and the results given in the text follow.

Measured Collisional Excitation Rate Coefficients for Oxygen VII*

R. C. ELTON

AND

W. W. KÖPPENDÖRFER†

Naval Research Laboratory, Washington, D. C.

(Received 20 February 1967)

Rate coefficients of $3.1 \times 10^{-11} \text{ cm}^3 \text{ sec}^{-1}$ and $1.5 \times 10^{-11} \text{ cm}^3 \text{ sec}^{-1}$ for collisional excitation of the $n=2$ singlet and triplet levels from the $1s^2 \ ^1S_0$ ground state in helium-like O VII have been determined within a factor of 2 in a plasma at an electron temperature of $kT = 250 \pm 60 \text{ eV}$ and density of $(6.2 \pm 1.5) \times 10^{16} \text{ cm}^{-3}$. The former compares favorably with a value of $(2.9 \pm 1.0) \times 10^{-11} \text{ cm}^3 \text{ sec}^{-1}$, calculated near threshold with an effective Gaunt factor of 0.2 for the same temperature. These coefficients have resulted from measurements on a θ -pinch device of the absolute intensity of the $1s2s \ ^3S_1 - 1s2s \ ^3P_{0,1,2}$ lines at 1639.6, 1638.0, and 1623.3 Å, respectively, and from relative measurements of the ratio of intensities for the $1s^2 \ ^1S_0 - 1s2p \ ^3P_1$ and $1s^2 \ ^1S_0 - 1s2p \ ^1P_1$ spectral lines at 21.8 Å and 21.6 Å respectively. Rate coefficients for the $2S - 2P$ singlet and triplet transitions and for the $1s2s \ ^3S_1 - 1s2s \ ^1S_0$ spin-exchange transitions have been calculated, as have the relevant transition probabilities. The measured oxygen concentration was $(0.6 \pm 0.2) \%$ in a deuterium plasma at an initial pressure of 60 mTorr. Considerations of radiative transfer are invoked to explain measurements over a long axial path length of a low intensity for the singlet resonance line at 21.6 Å, compared to the intercombination line at 21.8 Å.

I. INTRODUCTION

A KNOWLEDGE of cross sections for the excitation of ionic energy levels by charged particle impact is of prime importance in the spectroscopy of both

laboratory and astrophysical plasmas, which often exist in conditions that are far from those of thermodynamic equilibrium. In such instances, it is generally the highly ionized species of low atomic number that are involved. Often of equal importance is the collisional excitation rate coefficient, represented by the product of this cross section and the velocity of the colliding particle, averaged over the velocity distribution function. When multiplied by the product of the number

* Presented in part at the Conference on Ultraviolet and X-ray Spectroscopy of Laboratory and Astrophysical Plasmas, Culham, England (1966).

† Work performed while on leave from the Institut für Plasma-physik, Garching bei München, Germany.

densities of colliding particles, this coefficient represents the collisional excitation rate per unit volume for the levels considered.

Such rate coefficients are generally derived from calculated cross sections, since direct measurement by conventional methods involving beams are most often not feasible for ions. It is therefore the purpose of this paper to indicate by method and example how certain theoretically uncertain (e.g., for particle energies near the threshold for excitation) ionic rate coefficients may be determined experimentally through a measurement of line intensities and the use of transition probabilities and other reliably calculated (for transitions in which particle energies are much greater than the threshold energy and the Born and Bethe approximations hold) competing rate coefficients.

The resonance lines of the O VII ion in the helium isoelectronic sequence (Figs. 1 and 2) were chosen for detailed study. The importance of the radiation from this ion in the understanding of the structure of the solar corona through both absolute and relative (line ratio) intensity measurements is well established.¹ Of equal interest is the radiant flux emitted from oxygen ions in high-temperature laboratory plasmas.²⁻⁵ Line radiation from the heliumlike species N VI and C V has also been observed (Fig. 1), and is compared qualitatively with that of O VII.

The spectroscopic analysis leading to the desired rate coefficients is formulated in a framework describing a high-temperature ($kT = 250$ eV) transient plasma⁶ in a quiescent state with regard to particle density (prior to the onset of rapid end losses), but where the temperature is rising so rapidly that there exists no steady state coronalike equilibrium among ionic species. This is because radiative and three-body recombination rates are much less than the ionization and heating rates, which consequently control the ionic abundance. However, because the excitation and decay rates are large compared to the characteristic rate of change of abundance, the bound state densities can be described by steady-state relations, i.e., a balance between

collisional excitation and both radiative and collisional (only important for the $2S-2P$ transitions) de-excitation may be assumed.

The detailed analysis is limited to the ground state and $n=2$ levels, i.e., the direct effects of higher levels on the $n=2$ abundances has been neglected, because of the high radiative decay rates for excited electrons. Indirect population of the $n=2$ levels by cascading from higher levels, which are excited from the ground state, is considered and shown to be insignificant for the accuracies involved.

Thus, it is principally by the measurement of absolute and relative intensities of spectral lines and the consideration of all relevant processes that the desired excitation rates are determined. Referring to Fig. 2, the intensities of the O VII $1s2s\ ^3S_1-1s2p\ ^3P_{0,1,2}$ lines have been measured on an absolute scale and related to the total excitation rate coefficient

$$X(1^1S \rightarrow (2^3S + 2^3P))$$

for the triplet system. Unfortunately the corresponding 2^1S-2^1P line of the singlet system was not observable in O VII due to the dominance of the 1^1S-2^1P resonance line. However, a relative intensity measurement under optically thin conditions between the 1^1S-2^3P and 1^1S-2^1P lines was possible, which provided the necessary experimental information on the abundance in the $n=2$ singlet system and ultimately a determination of the equivalent singlet-rate coefficient

$$X(1^1S \rightarrow (2^1S + 2^1P)).$$

Because of the high ratio of length-to-diameter in the θ -pinch plasma used for these measurements, and the particular density-temperature conditions, observations under both optically thick (longitudinal) and optically thin (transverse) conditions were possible for the 1^1S-2^1P allowed-resonance line. The 1^1S-2^3P intercombination line was not, however, expected to become optically thick in either case, due to a much smaller oscillator strength.⁷ An exceptionally high ratio of measured intensities $I(1^1S-2^3P)/I(1^1S-2^1P)$ for these two lines when the plasma was viewed axially is explained through simple considerations of radiative transfer. The dependence of this ratio upon oxygen concentration and upon the element in the isoelectronic sequence is also analyzed.

Auxiliary measurements of the temperature, densities, and plasma dimensions required in the analysis were obtained spectroscopically⁶ (simultaneous with the 2^3S-2^3P intensity measurements) from continuum emission of the deuterium plasma in the visible and soft x-ray spectral regions, as well as from observations of the time resolved intensities of O III-O VIII impurity line radiation, interpreted in terms of electron temperature through calculated ionization relaxation times. Independent support for the temperature used is gained from a simultaneous measurement of the

¹ R. L. Blake, T. A. Chubb, H. Friedman, and A. E. Unzicker, *Astrophys. J.* **142**, 1 (1965).

² B. Edlen, *Physica* **13**, 545 (1947); *Arkiv Fysik* **4**, 441 (1951).

³ B. C. Fawcett, A. H. Gabriel, W. G. Griffin, B. B. Jones, and R. Wilson, *Nature* **200**, 1304 (1963).

⁴ G. A. Sawyer, A. J. Bearden, I. Henins, F. C. Jahoda, and F. L. Ribe, *Phys. Rev.* **131**, 1891 (1963). See also F. C. Jahoda, F. L. Ribe, G. A. Sawyer, and R. W. P. McWhirter, in *Proceedings of the Sixth International Conference on Ionization Phenomena in Gases, Paris, 1963* (S.E.R.M.A., Paris, 1964).

⁵ R. C. Elton, E. Hintz, and M. Swartz, in *Proceedings of the Seventh International Conference on Phenomena in Ionized Gases* (Gradevinska Knjiga Publishing House, Belgrade, 1966), Vol. 3, p. 190.

⁶ A. C. Kolb, W. H. Lupton, R. C. Elton, E. A. McLean, M. Swartz, M. P. Young, H. R. Griem, and E. Hintz, *Plasma Physics and Controlled Nuclear Fusion Research* (International Atomic Energy Agency, Vienna, 1966), Vol. 1, p. 261. The percent oxygen concentration reported here and in Ref. 5 of 0.15 has now been corrected to be 0.6, and the reported electron densities reduced 12% by corrections for a contribution to the measured continuum radiation from oxygen-ion bremsstrahlung (carbon negligible).

⁷ R. C. Elton, *Astrophys. J.* **148**, 573 (1967).

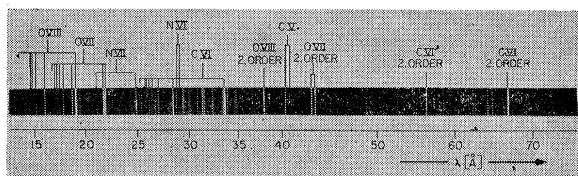


FIG. 1. Time-integrated spectrum from the θ -pinch device viewed axially. The spectrum represents a superposition of 20 discharges. (Angle of incidence = 87.5° , 576-groove/mm glass grating with a 2.2-m radius of curvature.)

electron temperature above 300 eV from the x-ray continuum radiation.^{5,6}

II. DESCRIPTION OF EXPERIMENT AND MEASUREMENTS

Plasma Source

The source of radiation for these measurements was a plasma generated in a θ -pinch device⁶ storing 640 kJ of energy at 18 kV. Deuterium at an initial pressure of 60 mTorr is initially ionized in the presence of a reverse bias field which slowly rises to -5.8 kG. The main field rises to a maximum of 50 kG in 10 μ sec producing temperatures as high as 400 eV and peak electron densities of $\sim 10^{17}$ cm^{-3} . The cylindrical plasma generated has a length of ~ 100 cm and a diameter of ~ 2 cm at midplane, tapering down near the ends due to the shape of the confining field. At the time (~ 6 μ sec after initiation of the discharge) the lines of interest are emitted, the density is approaching maximum prior to the onset of a rapid end-loss flux and the temperature is in the region of $kT = 250$ eV and rising. All of the emitted line radiation stems from intrinsic or added impurities. These and other properties of the plasma have been described previously.^{5,6}

Spectroscopic Instrumentation

Absolute time-resolved measurements of the intensity of the $2^3S_1-2^3P_{0,1,2}$ lines⁷ of O VII at 1639.6, 1638.0, and 1623.3 \AA , respectively, were carried out with a 0.5-m Seya-Namioka-type vacuum spectrograph. For calibration, the relative efficiency of this instrument was determined with a monochromatic beam obtained from a second vacuum monochromator. The detector consisted of a lumogen⁸ phosphor and photomultiplier combination calibrated at 3889 \AA with a standard tungsten ribbon lamp. (Further details of the calibration procedure are described elsewhere.^{5,9})

The radiation emitted in the soft x-ray region of the spectrum at 21.6 \AA and 21.8 \AA , for the 1^1S-2^1P and 1^1S-2^3P lines of O VII respectively, was detected both photographically and photoelectrically with a 2.2-m grazing incidence combination vacuum spectrograph and scanning monochromator, operated at

⁸ N. Kristianpoller and D. Dutton, Appl. Optics **3**, 287 (1964).

⁹ R. C. Elton, in Proceedings of the Symposium on Interdisciplinary Aspects of Radiative Energy Transfer, Philadelphia, Pennsylvania, 1966 (to be published in J. Quant. Spectry. Radiative Transfer, 1968).

an angle of incidence of 87.5° . A typical plate (SWR emulsion) obtained over 20 discharges using a grating with 576 grooves/mm ruled lightly on glass¹⁰ is shown in Fig. 1. An entrance slit of 0.01 mm was used in this case. For photoelectric measurements, a plastic scintillator in combination with a photomultiplier was used as detector.

For photographic and photoelectric measurements perpendicular to the axis of the plasma column, a rectangular extension, which projected radially outward between coil sections with an opening to the plasma of 4 mm wide by 12 mm high, was added to the quartz θ -pinch container. No effect on the macroscopic behavior of the discharge was noted in operation with this port.

III. ANALYSIS OF THE SPECTROSCOPIC OBSERVATIONS

The intensity of a spectral line associated with a transition originating in a $2P$ upper level may be written

$$p(\eta S-2P) = n(1S) h\nu A(\eta S-2P) [n(2P)/n(1S)], \quad (1)$$

where $n(1S)$ and $n(2P)$ are the population densities of the respective levels and where η is the principal quantum number of the lower state (either 1 or 2).

Solution of the Rate Equations

The dependence of the ratio $n(2P)/n(2S)$ on the desired excitation rate coefficients is obtained from a detailed consideration of the rate equations for constant electron density ($dn_e/dt \approx 0$ at the time of peak O VII signals) in terms of transition probabilities A and electron¹¹ impact excitation rates $n_e X$ for the transitions shown in Fig. 2. Primes are used in this section to distinguish the triplet system from the unprimed singlet levels.

For the triplet system, the rate equations may be written:

$$\begin{aligned} dn(2P')/dt = & n(1S)n_e X(1S-2P') \\ & + n(2S')n_e X(2S'-2P') - n(2P')\Pi' \equiv 0, \quad (2) \end{aligned}$$

and

$$\begin{aligned} dn(2S')/dt = & n(1S)n_e X(1S-2S') + n(2P')\zeta'\Pi' \\ & + n(2S)n_e X(2S'-2S)[g(2S')/g(2S)] \\ & - n(2S')n_e X(2S'-C) - n(2S')n_e X(2S'-2P') \\ & - n(2S')n_e X(2S'-2S) \equiv 0, \quad (3) \end{aligned}$$

where the positive terms represent population rates and the negative terms depopulation rates. The rate coefficients $X(2S'-C)$ and $X(2P'-C)$ represent transitions to continuum states beyond the thermal limit¹² from

¹⁰ The authors are indebted to Professor Manne Siegbahn of the Nobelinstitut för Physik, Stockholm for providing us with the special grating used for these measurements.

¹¹ Because of their large velocities, it generally suffices only to consider excitation by collisions with electrons. For $2S-2P$ transitions, excitation by ions may become comparable.

¹² R. Wilson, J. Quant. Spectry Radiative Transfer **2**, 477 (1962).

which decay corresponds to recombination. Also, the total $2P'$ depopulation rate is represented here by

$$\Pi' = A(1S-2P') + A(2S'-2P') + n_e X(2S'-2P') [g(2S')/g(2P')] + n_e X(2P'-C), \quad (4)$$

while the fractional rate into the $2S'$ level is denoted by

$$\zeta' = \{A(2S'-2P') + n_e X(2S'-2P') [g(2S')/g(2P')]\} / \Pi'. \quad (5)$$

A similar set of equations can be written for the singlet system by reversing the signs on the two terms involving $n=2$ exchange transitions and by adding (and removing) primes on the remaining $n=2$ term designations. The corresponding singlet-parameter ζ may readily be neglected due to a transition rate from the $2P$ level into the ground-state $A(1S-2P)$ about four orders of magnitude greater than alternate de-excitation mechanisms. Similarly, Π may be approximated by $A(1S-2P)$ in what follows.

The terms on the right-hand side in the rate equations, as determined from the rates given in Table II, are much greater than the rates of change in density of the $n=2$ levels, e.g., $dn(2P')/dt$, particularly at peak signal and near-peak electron density. Therefore, it is reasonable to set the rate equations equal to zero, so that the resulting relations represent a steady-state balance between population and depopulation rates for transitions affecting the $n=2$ levels.

In these equations the collisional deexcitation rates are expressed in terms of the corresponding excitation rates through detailed balancing, with g representing the statistical weight of a particular level. Collisional depopulation into the ground state is negligible compared to radiative decay because of a density of $n=2$ states much lower than that of the ground state. Concerning the $n=2$ intercombination transitions involving electron

spin change, the simplifying assumption made here is that the only significant transitions are between the 2^3S and the 2^1S levels, involving s -wave electrons.

Population of the $n=2$ levels by the cascading of recombining electrons can be neglected here, since the temperature is rising and the plasma is not in a steady state with regard to ionic species, i.e., during the heating phase of a transient plasma a particular ionization state is present at higher electron temperatures than would correspond to corona equilibrium. Therefore ionization rates ($\sim 10^6 \text{ sec}^{-1}$) and electron impact excitation rates (Table II) dominate recombination rates ($\sim 10^4 \text{ sec}^{-1}$), which decrease with higher temperatures.^{5,18}

Finally, concerning the effect of higher bound states below the thermal limit, the high rate for radiative decay ($\sim 10^{10} \text{ sec}^{-1}$) from these levels permits the neglect of depopulation from the $n=2$ states by collisional excitation to states of higher-principal quantum number and also the neglect of ionization by step-wise excitation. Additional population of the $n=2$ levels from the ground state indirectly through cascading from higher bound states is neglected here, since it is reasonable to expect the cross section for excitation from the ground state to scale as the oscillator strength and inversely as the excitation energy [Eq. (10)]. Therefore only the 3^1P and 3^3P levels with $f(1S-3P) = 0.15$ and $\Delta E = 660 \text{ eV}$ are likely to be effective and could cause a reduction in the measured results for excitation rates into the $n=2$ levels direct from the ground state by about 12% which is negligible compared to the over-all accuracy of this analysis.

By relating the singlet $n=2$ population to the triplet through the measured optically thin intensity ratio

$$\rho \equiv \dot{p}(1S-2P) / \dot{p}(1S-2P'), \quad (6)$$

the four rate equations may be solved for both $n_e X(1S \rightarrow (2S+2P))$ and $n_e X(1S \rightarrow (2S'+2P'))$ in terms of $n(2P')/n(1S)$ which, with Eq. (1), yields

$$n_e X(1S \rightarrow (2S+2P)) \approx \left(\frac{1+R}{1+\beta+\gamma+R} \right) \frac{1}{n(1S)} \left[\frac{\dot{p}}{h\nu A} (2S'-2P') \right] \left[\rho(1+\beta+\gamma) A(1S-2P') - \gamma \Pi' \left(\frac{\zeta'+R'}{1+\beta'+\gamma'+R'} \right) \right], \quad (7)$$

and

$$n_e X(1S \rightarrow (2S'+2P')) \approx \left(\frac{1+R'}{1+\beta'+\gamma'+R'} \right) \frac{1}{n(1S)} \left[\frac{\dot{p}}{h\nu A} (2S'-2P') \right] \times \left[(1+\beta'+\gamma'-\zeta') \Pi' - \gamma \rho \left(\frac{R}{1+\beta+\gamma+R} \right) A(1S-2P') \right], \quad (8)$$

in the limits of $X(2S-2P) \approx X(2S'-2P')$, $\nu(1S-2P) \approx \nu(1S-2P')$, and $\gamma\gamma'/(1+\beta+\gamma)(1+\beta'+\gamma') \ll 1$. Here the abbreviations

$$\beta \equiv X(2S-C)/X(2S-2P),$$

$$\beta' \equiv X(2S'-C)/X(2S-2P),$$

$$\gamma \equiv X(2S'-2S) [g(2S')/g(2S)] / X(2S-2P),$$

$$\gamma' \equiv X(2S'-2S) / X(2S-2P),$$

and

$$R \equiv X(1S-2S) / X(1S-2P),$$

$$R' \equiv X(1S-2S') / X(1S-2P') \quad (9)$$

have been introduced.

¹⁸ H. R. Griem, *Plasma Spectroscopy* (McGraw-Hill Book Company, Inc., New York, 1964).

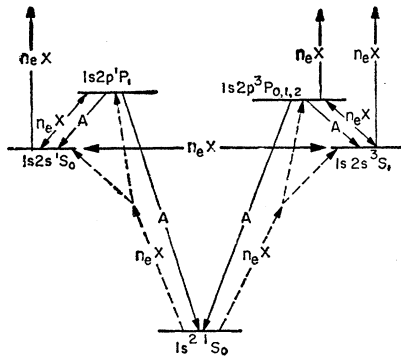


FIG. 2. Diagram of energy levels in O VII relevant to the present analysis. The transition probabilities A and excitation rates $n_e X$ accompanying solid lines are calculated; excitation rates associated with dashed lines are measured.

The presence of the ratios R and R' in Eqs. (7) and (8) is due to an allowance for a noncomplete equilibrium distribution of populations between the $2S$ and $2P$ levels in the respective systems. For strong $2S-2P$ coupling β, β', γ , and γ' approach zero in these relations and the dependence upon R and R' is removed, which is equivalent to considering the $2S$ and $2P$ levels degenerate in the analysis. The resulting expressions are identical to those obtained from a pure coronal model with the exception of terms in $n_e X(2S'-2S)$, which occur explicitly in the product $\gamma\Pi'$ and which ultimately disappear in the low-density limit.

Determination of $X(1^1S \rightarrow (2^1S+2^1P))$ and $X(1^1S \rightarrow (2^3S+2^3P))$

From O VII transition rates calculated below and listed in Table II, from the measured radiant power density $p(2^3S-2^3P) = 90 \pm 40$ W/cm³ (for the entire multiplet), and from a measured ratio of 2.5 ± 0.5 between the singlet and triplet resonance line intensities, it is now possible to determine, using Eqs. (1), (7), and (8), the total excitation rate coefficients into the $n=2$ levels from the ground state, i.e., $X(1^1S \rightarrow (2^1S+2^1P))$ and $X(1^1S \rightarrow (2^3S+2^3P))$. Using nominal values, these are found to be 3.1×10^{-11} cm³ sec⁻¹ and 1.5×10^{-11} cm³ sec⁻¹ respectively (in the ratio of ~ 2 to 1) and listed in Table I. For this a value of $n(1S)$ of $(1.9 \pm 0.6) \times 10^{14}$ cm⁻³ was determined from a measured electron density of $(6.2 \pm 1.5) \times 10^{16}$ cm⁻³ and a total percent oxygen concentration^{5,6} of (0.6 ± 0.2) , of which $\sim 50\%$ is O VII at the time of interest as evidenced by relative intensity measurements between the O VIII Lyman- α line at 18.9 Å and the O VII resonance series lines. (O VI has completely disappeared at the time of peak O VII emission.)

The ratio R defined in Eq. (9) is assumed here to be 0.28 from data for hydrogenic ions.^{14,15} The same ratio for the triplet system, designated by R' , is assumed to

¹⁴ J. Tully, M. Sc. dissertation, London, 1960 (unpublished). See also Ref. 17.

¹⁵ A. Burgess, Mem. Soc. Roy. Sci. Liege 4, 299 (1961). See also Ref. 17.

be 0.3 according to a final distribution among excited states in the ratio of statistical weights. This latter assumption is expected to be valid for the close-coupling interactions in O VII with electron energies near the threshold for excitation.

The experimental uncertainties given above introduce an over-all accuracy for $X(1^1S \rightarrow (2^1S+2^1P))$ and $X(1^1S \rightarrow (2^3S+2^3P))$ of a factor of 2. Additional uncertainties due to the calculated quantities involved are negligible, since the major uncertainties are in $X(2^2S-2^1S)$, $X(2^1S-C)$, $X(2^3S-C)$, and $X(2^3P-C)$, all of which enter only weakly¹⁶ for O VII. The effect on the final results of uncertainties in R and R' is also negligible compared to the experimental uncertainties.

That the total singlet-rate coefficient arrived at here is of reasonable value is seen from an estimate for $n_e X(1^1S-2^1P)$ of 1.4×10^6 sec⁻¹, as calculated from the formula given below for allowed transitions, expected to be reliable approximately to a factor of 2 near threshold.^{17,18} This value, when multiplied by $R+1$ and divided by n_e , yields a calculated estimate (for $kT = 250 \pm 60$ eV) of

$$X(1^1S \rightarrow (2^1S+2^1P)) = (2.9 \pm 1.0) \times 10^{-11} \text{ cm}^3 \text{ sec}^{-1},$$

also listed in Table I for comparison.

Variations in $p(1^1S-2^1P)/p(1^1S-2^3P)$

The ratio of resonance line intensities ρ , defined in Eq. (6) and which may be expressed in terms of atomic constants through the use of Eqs. (7) and (8), depends upon electron density and in addition has a marked dependence upon ionic charge, i.e., for constant electron density, the ratio increases towards lighter elements along the helium isoelectronic sequence. This effect can be seen in Fig. 1 for O VII, N VI, and C V and is due both to a decrease in the intercombination line oscillator strength⁷ and to an increase in cross sections for collisional depopulation of the $n=2$ triplet levels. A further dependence upon temperature (and therefore ionic species), as well as a dependence of this ratio upon concentration of radiating ions, is encountered when the

TABLE I. Resulting collisional excitation rate coefficients X per O VII ion for $kT = 250 \pm 60$ eV. The measurements are accurate to within a factor of 2.

Transitions	X (Measured) [cm ³ sec ⁻¹]	X (Calculated) ^a [cm ³ sec ⁻¹]
$1^1S \rightarrow (2^1S+2^1P)$	3.1×10^{-11}	$(2.9 \pm 1.0) \times 10^{-11}$
$1^1S \rightarrow (2^3S+2^3P)$	1.5×10^{-11}	

^a The variation shown is calculated from the temperature uncertainty.

¹⁶ The singlet- and triplet-excitation rates were evaluated from Eqs. (7) and (8) for a range of values for $X(2^3S-2^1S)$ of zero to $X(2^3S-2^3P)$, i.e., $\gamma' = 0$ to 1, and found to produce a typical maximum deviation from the nominal values reported in Table I of $\pm 15\%$. The effect on the ratio is more pronounced.

¹⁷ M. J. Seaton, in *Atomic and Molecular Processes*, edited by D. R. Bates (Academic Press Inc., New York, 1962), Chap. 11.

¹⁸ H. Van Regemortel, *Astrophys. J.* **136**, 906 (1962).

radiation is emitted from optically dense layers. Such additional effects may only be understood through considerations of radiative transfer as discussed in Sec. V below.

IV. EXCITATION RATE COEFFICIENTS AND TRANSITION PROBABILITIES EMPLOYED

The analysis described above is based upon the calculated excitation and deexcitation rates listed in Table II for the relevant transitions illustrated in Fig. 2.

Excitation Rate Coefficients

Allowed Transitions

For the optically allowed transitions, excitation cross sections σ_a have been calculated from the Bethe approximation formula^{18,17-19}

$$\sigma_a = 4\pi^2 e^4 f \bar{G} / m v^2 \Delta E \sqrt{3}, \quad (10)$$

considered particularly valid for electron energies above threshold (Born approximation limit), and also considered reliable to within a factor of 2 near threshold, through the use of effective Gaunt factors \bar{G} for positive ions.¹⁷⁻¹⁹ The quantities f and ΔE are respectively the absorption oscillator strength and the difference in excitation energy between levels; e , m , and v represent the electron charge, mass and velocity.

For the singlet-resonance transition (1^1S-2^1P) with $\Delta E=570$ eV and $3kT/2=375$ eV, as well as for the 2^1S-C , 2^3S-C , and 2^3P-C transitions (which do not enter strongly for O VII), where $\Delta E=420$ eV as given⁶ approximately by the ionization energy interval plus kT , \bar{G} was taken equal to 0.2. However, for the 2^1S-2^1P and 2^3S-2^3P transitions ($\Delta E \approx 7$ eV), a value of $\bar{G}=1.0$ was used.

The excitation rate per ion $n_e X = \langle \sigma v \rangle n_e$ is found by averaging¹⁸ over a Maxwellian velocity distribution to be

$$n_e X = (2\pi/3mkT)^{1/2} (4\pi e^4 \bar{G} n_e / \Delta E) \exp(-\Delta E/kT), \quad (11)$$

which yields the values given in Table II for the allowed transitions. The electron density n_e and temperature T (averaged over the length of the discharge), are known to within $\pm 25\%$ from independent measurements.^{5,6}

Spin Exchange Transitions

Accurate theoretical estimates for the excitation rate coefficients for the $n=2$ intercombination transitions involving electron spin exchange (namely 2^3S-2^1S , 2^3P-2^1P , 2^1S-2^3P , and 2^3S-2^1P)—all involving a change in multiplicity—are not available. The first two transitions, which involve no change in azimuthal quantum number l , are considered the most probable, and of these two, the interaction with s -wave electrons

¹⁹ C. W. Allen, *Astrophysical Quantities* (The Athlone Press, London, 1963), 2nd ed.

TABLE II. Estimated transition probabilities A and excitation rates $n_e X$ per O VII ion appropriate to the spectroscopic analysis, with $n_e = 6.2 \times 10^{16}$ cm⁻³ and $kT = 250$ eV.

Transition	f	$n_e X$ [sec ⁻¹]	A [sec ⁻¹]
$1^1S_0-2^1P_1$	0.69	1.4×10^6	3.3×10^{12}
$1^1S_0-2^3P_{0,1,2}$	1.1×10^{-4}		1.7×10^8
$2^1S_0-2^1P_1$	0.068	7.0×10^8	
$2^3S_1-2^3P_{0,1,2}$	0.095	7.0×10^8	0.79×10^8
$2^1S, 2^3S, 2^3P \rightarrow C$	0.15	2.2×10^6	
2^3S-2^1S		1.1×10^8	

(i.e., head-on collisions with vanishing incident angular momentum) is expected to give the highest exchange rate.²⁰ Concerning this 2^3S-2^1S transition,²¹ measurements of Phelps²² at low (300°K) temperatures indicate that the cross section per electron for helium is near the theoretical inelastic maximum for s waves, i.e., the relative angular momentum is restricted to $mv\rho_{\max} = \hbar$ and

$$\sigma_s \approx \pi \rho_{\max}^2 \approx \pi (\hbar/mv)^2, \quad (12)$$

where ρ_{\max} is the maximum impact parameter and v represents the relative velocity. Again for helium, the $2s$ orbit has a characteristic dimension of $\sim 4a_0 \approx 2 \times 10^{-8}$ cm, and ρ_{\max} for thermal electrons is about the same. Since velocities scale essentially inversely as the ionic charge (minus one), both ρ_{\max} and the size of the characteristic orbit scale similarly throughout the isoelectronic sequence. Thus the probability of exchange between continuum s electrons and bound $2s$ electrons should also remain unchanged. Equation (12) should therefore be reasonably reliable for O VII as well, and is considered to be somewhat of an upper limit for this exchange rate.

Additional information is gained by writing^{18,19} the cross section in terms of the ratio of the collision strength Ω to the statistical weight of the initial level g_i :

$$\sigma_s = \pi (\hbar/mv)^2 (\Omega/g_i). \quad (13)$$

This is identical, for a ratio $\Omega/g_i=1$, to the maximum value given in Eq. (12) which, if a reasonable¹⁹ value for Ω of unity is assumed, is obtained for collisional deexcitation transitions from the 2^1S to the 2^3S level ($g_i=1$), i.e., $g_i \sigma_s \approx \sigma_s(\max)$.

Therefore, Eq. (12) is used in determining the total s -wave exchange rate, so that the excitation cross section $\sigma(2^3S \rightarrow 2^1S)$ is given by σ_s/g_i (averaged according to statistical weights) and the excitation rate becomes

$$n_e X(2^3S \rightarrow 2^1S) = (2\pi m/9kT)^{1/2} (\hbar/m)^2 n_e. \quad (14)$$

This equation yields a value of 1.1×10^8 sec⁻¹ per ion and a value for γ' of 0.15. A value for γ' less than

²⁰ H. S. W. Massey and E. H. S. Burhop, *Electronic and Ionic Impact Phenomena* (Oxford University Press, London, 1952).

²¹ The authors are indebted to Professor H. R. Griem for this analysis leading to the extrapolated estimate for $\sigma(2^3S-2^1S)$.

²² A. V. Phelps, *Phys. Rev.* **99**, 1307 (1955).

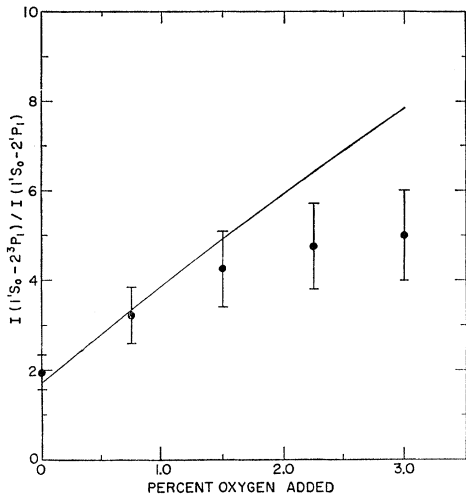


FIG. 3. Ratio of axial intensities for the 1^1S-2^3P and 1^1S-2^1P lines of O VII versus percent oxygen added to the deuterium fill pressure of 60 mTorr. The curve, calculated from Eq. (16), has been reduced 10% to fit the experimental points at low concentrations for comparison. The deviation at high concentrations is attributed to a slight drop in temperature.

unity is consistent with the observation of lines from triplet transitions at least several orders of magnitude stronger than unobservable equivalent singlet lines, which indicates a reasonable decoupling of the two systems since a dominating collisional exchange rate would rapidly depopulate the triplet levels through the allowed resonance transition.

Transition Probabilities

The transition probabilities for radiative decay were calculated¹³ to an expected accuracy of $\pm 5\%$ for the allowed lines and to within $\pm 20\%$ for the 1^1S-2^3P intercombination line, using the corresponding calculated absorption oscillator strengths.^{7,23}

V. CONSIDERATIONS OF RADIATIVE TRANSFER FOR AXIAL OBSERVATIONS

Viewing the plasma axially, the intensity of the optically thin $1^1S_0-2^3P_1$ intercombination line of O VII has been found to be greater than that of the optically thick allowed $1^1S_0-2^1P_1$ line, which is just the opposite to that observed in side-on measurement (used for the above analysis) where the resonance line is optically thin, as well as in the solar corona. In addition, a further increase in the intensity of the intercombination line relative to the allowed singlet line with increased oxygen content is not understood from the above analysis for optically thin conditions. It is the purpose of this section to present a plausible explanation for these observations, based upon considerations of radiative transfer.

²³ Natl. Std. Ref. Data Ser. Natl. Bur. Std. (U.S.) NSRDS-NBS-4 (1966).

In the simplest case of a uniform plasma²⁴ with a constant source function S over the length viewed, the solution to the equation of radiative transfer is given by

$$I_\nu = S[1 - \exp(-\tau)]. \quad (15)$$

Assuming the resonance lines are broadened only by the Doppler effect, the ratio of intensities may be written as²⁵

$$\frac{I(1^1S-2^3P)}{I(1^1S-2^1P)} = \Lambda \frac{\rho(1^1S-2^3P)}{\rho(1^1S-2^1P)}, \quad (16)$$

where $\rho(1^1S-2^3P)/\rho(1^1S-2^1P)$ is the optically thin intensity ratio and where

$$\Lambda \equiv \tau_c \pi^{1/2} \Delta\nu \int_{-\infty}^{+\infty} d\nu \left\{ 1 - \exp \left[-\tau_c \exp \left(-\frac{(\nu - \nu_0)^2}{\Delta\nu^2} \right) \right] \right\} \quad (17)$$

is a function of τ_c , the optical depth at the center of the 1^1S-2^1P line. Here $\Delta\nu$ is the Doppler width at the $1/e$ intensity level. For the conditions defined in the above analysis τ_c is found¹³ to be 9 ± 3 with a corresponding value²⁶ for Λ of 5 ± 1 . Combining this with a value for $\rho(1^1S-2^3P)/\rho(1^1S-2^1P)$ of 0.4 ± 0.1 (as obtained from side-on measurements) according to Eq. (16) produces a nominal expected intensity ratio

$$I(1^1S-2^3P)/I(1^1S-2^1P)$$

for axial observation of 2 ± 1 . Measurement of this ratio for the same concentration yields a value of 2.0 ± 0.4 (see Fig. 3) which is in remarkably good agreement.

Also, the parameter Λ is a function of the oxygen

TABLE III. Λ as a function of τ_c (the peak optical depth of the Doppler-broadened 1^1S-2^1P line).

τ_c	Λ
0.1	1.04
0.2	1.07
0.5	1.18
1	1.38
2	1.80
5	3.16
10	5.38
20	9.50
40	17.4
60	25.0
80	36.8
100	38.8

²⁴ The existence of a temperature gradient at the end of the discharge, sufficient to cause absorption of an appreciable fraction of the allowed $1^1S_0-2^1P_1$ line intensity, is unlikely because of the limited temperature regime in which O VII ions are present.

²⁵ A. C. G. Mitchell and M. W. Zemansky, *Resonance Radiation and Excited Atoms* (Cambridge University Press, New York, 1961), Appendix V. The inclusion of additional effects due to resonance scattering of the absorbed radiation radially outward has been considered by one of us (WWK) and found to affect the source function by a negligible amount (less than 30%) for a long cylinder with a radial optical depth less than 0.3.

concentration through τ_c , which produces a dependence not present in the optically thin analysis above. This is shown in Fig. 3 where the ratio $I(1^1S-2^3P)/I(1^1S-2^1P)$ is plotted versus the percentage of oxygen added to the normal 0.6% volume concentration. Also plotted on this graph for comparison is the ratio calculated from Eq. (16), adjusted to fit the data at 0.75% concentration. Values for Λ used were numerically calculated for the increased optical depths and are given in Table III. The deviation at higher concentrations is due to a drop in intensity for the 1^1S-2^3P line as the temperature decreases at high impurity content.^{5,6}

The function Λ is also temperature sensitive which implies a sensitivity to Z , i.e., the element along the isoelectronic sequence, in addition to that discussed in the optically thin analysis above. This effect is in such a direction as to increase Λ and effectively enhance the intensity of the optically thin lines relative to the optically thick lines as temperature (and Z) rises.

VI. SUMMARY AND CONCLUSIONS

The measurement of 2^3S-2^3P line radiation which is intense compared to that for the corresponding singlet system, as well as the observation of a relatively strong 1^1S-2^3P intercombination line, has led for the plasma conditions present in the θ -pinch discharge used both to the hypothesis of rather weak singlet-triplet collisional coupling in oxygen-VII at the $n=2$ level and ultimately to a determination of comparable rate coefficients (Table I) for excitation of the $n=2$ singlet and triplet levels from the ground state. The analysis has been carried out for intermediate collisional coupling between the $2S$ and $2P$ levels in each system, allowing for excitation into higher states beyond the thermal limit and for transitions to the alternate systems through 2^3S-2^1S exchange collisions. The effect of additional indirect population by cascading from levels of higher principal quantum number, excited from the ground state, has been considered and shown to be of minor significance to the quantitative results. Population by recombination from O VIII has been neglected in the analysis, since the temperature is rising rapidly and the plasma is not in a steady state with regard to ionic species.

The limitation in accuracy to a factor of 2 in the final results is due mainly to an accumulation of experimental uncertainties, since the calculated transition probabilities and excitation rates used in the analysis either are quite accurate or enter insensitively.

The measured value for the singlet excitation rate coefficient given in Table I compares very well with a value (also listed) calculated using an effective Gaunt factor of 0.2 from a formula considered reliable for electron energies above the threshold energy for excitation, i.e., in the region of validity of the Born and Bethe approximations, but previously only considered reliable to a factor of 2 near threshold. (The accuracy shown for the calculated value in Table I reflects the effect of a $\pm 30\%$ uncertainty in temperature.) Within the limitations of the combined accuracies, the formula appears to be reliable for transitions near threshold as well.

The observation of a low intensity for the 1^1S-2^1P resonance line compared to the 1^1S-2^3P intercombination line, when the plasma was viewed axially over a long path length, is in contradiction to that from radial observations, where the plasma is optically thin for this radiation. The results are reported above and explained through simple considerations of radiative transfer.

In conclusion, a method has been described for obtaining values for impact excitation rate coefficients for transitions near threshold in ions present in both laboratory and astrophysical plasmas, through a measurement of absolute and relative line intensities and the use of more certain rate coefficients and transition probabilities. The particular example of excitation into the $n=2$ singlet and triplet levels of O VII is described. The chief results are the measurement of values for the singlet and triplet resonance rate coefficients in a ratio of approximately 2:1 and a singlet rate coefficient in excellent agreement with that calculated from a formula previously considered reliable only far above threshold. The present accuracy is limited mainly by uncertainties in the experimental measurements of intensity and in the knowledge of plasma conditions. Improvements here could eventually result in uncertainties of as low as $\pm 30\%$ for such measurements.

ACKNOWLEDGMENTS

The authors are most grateful to Professor H. R. Griem of the University of Maryland for many discussions and valuable suggestions, particularly in obtaining an estimate for the 2^1S-2^3S exchange rate coefficient. The continued interest and constant encouragement of Dr. A. C. Kolb is also graciously acknowledged. The technical assistance of E. Laikin in the operation of the θ -pinch device and of J. L. Ford in obtaining the spectroscopic data is greatly appreciated.

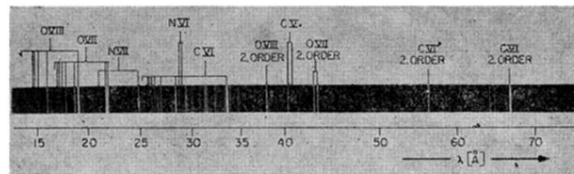


FIG. 1. Time-integrated spectrum from the θ -pinch device viewed axially. The spectrum represents a superposition of 20 discharges. (Angle of incidence = 87.5° , 576-groove/mm glass grating with a 2.2-m radius of curvature.)